The Journal of Neuroscience, May 1995, 15(5): 3612–3621

Electrogenic Na-Ca Exchange Clears Ca^{2+} Loads from Retinal Amacrine Cells in Culture

Evanna Gleason,[a] Salvador Borges, and Martin Wilson

Division of Biological Sciences, Section of Neurobiology, Physiology and Behavior, University of California, Davis, California 95616

Calcium influx into cultured retinal amacrine cells is followed by a small, slow, inward current that we show here results from the operation of electrogenic Na-Ca exchange. The activity of the exchanger is shown to correlate with the magnitude of the Ca^{2+} load and to depend on both the Ca^{2+} and Na^+ gradients. Li^+ is unable to substitute for Na^+ and in the absence of Na^+, slow tail currents are almost entirely suppressed. A rapid change in $[K^+]_o$ does not affect the activity of the exchanger, suggesting that only Na^+ and Ca^{2+} are transported. The ratio of charge entering as Ca^{2+} current to the charge entering as exchange current is highly variable between cells. We suggest that variability results from a variable fraction of Ca^{2+} load, we estimate typically 40%, being removed by a process other than Na-Ca exchange. This process is likely to involve internal buffering or sequestration since inhibition of the plasmalemmal Ca^{2+}-ATPase does not increase the fraction of Ca^{2+} expelled by the exchanger. Ca^{2+} loading performed in the absence of Na^+_o generates smaller exchange charge the longer the delay in returning Na^+_o to the neuron. About 30% of exchange charge is lost for a delay of 1 sec.

[Key words: Na-Ca exchange, Ca-ATPase, calcium current, amacrine cell, retina, patch clamp]

Calcium entry into cells triggers numerous processes. Foremost among these in neurons is the release of neurotransmitter (Katz and Miledi, 1967; Smith and Augustine, 1988). Equally as important as Ca^{2+} entry is the subsequent return of cytosolic Ca^{2+} to resting levels. Intracellular Ca^{2+} can be temporarily sequestered by organelles or buffered by Ca^{2+} binding proteins but ultimately excess Ca^{2+} must be exported from the cell. The two known mechanisms for Ca^{2+} extrusion are the plasma membrane Ca^{2+}-ATPase (Carafoli, 1991) and the Na-Ca exchanger (DiPolo, 1989; Eisner and Lederer, 1989; Lagnado and McNaughton, 1989, 1990; McNaughton, 1991). The functional distinctions between these two mechanisms have been established in the squid axon (Dipolo and Beauge, 1979, 1983) where the two systems are thought to be complementary. The Ca^{2+}-ATPase has a high affinity for Ca^{2+} but low flux capacity, whereas Na-Ca exchange has a low affinity for Ca^{2+} but a high capacity. These properties suggest that the Ca^{2+}-ATPase functions primarily in recovery from small Ca^{2+} loads and maintenance of resting Ca^{2+} while the Na-Ca exchanger is important for removing large Ca^{2+} loads as would be produced by trains of action potentials or prolonged depolarizations. The removal of Ca^{2+} introduced by the latter condition is a significant challenge for retinal amacrine cells in particular because their membrane properties allow them to support sustained graded potentials (Werblin and Dowling, 1969; Eliasof et al., 1987).

Sodium–calcium exchange is thought to be electrogenic by virtue of an inequality in the number of charges leaving and entering the cell with every Ca^{2+} expelled. The small current generated by this inequality has been described in both cardiac myocytes (Kimura et al., 1986; Mechman and Pott, 1986) and rod outer segments (Yau and Nakatani, 1984). In both of these preparations this small current has provided a very valuable assay of exchanger activity (Ehara et al., 1989; Cervetto et al., 1989). Here we demonstrate directly that the Na-Ca exchange mechanism for a more typical vertebrate CNS neuron is also electrogenic. We then use this current to assess the role Na-Ca exchange plays in clearing Ca^{2+} loads in these cells.

Materials and Methods

Cultures

Retinal neurons were dissociated from chick embryos and cultured by methods described previously (Gleason et al., 1993). Cells were maintained in Dulbecco's Modified Eagle's Medium (Sigma), supplemented with 5% fetal calf serum (HyClone), 100 U/ml penicillin/streptomycin and 400 μM glutamine. Amacrine cells were identified by their morphology (Huba and Hoffmann, 1990; Gleason et al., 1993) and were used after 6–10 d in culture.

Solutions

In most experiments solutions were changed by gravity-flow superfusion of the cell from a 1 mm diameter inlet tube positioned nearby. For switching external K^+ solutions or for switching between Na^+-containing and Na^+-free solutions, superfusion was achieved by having two parallel laminar streams of solution flowing from two tubes of either 300 or 1000 μm diam. close to the cell. Moving the assembly holding the tubes caused the boundary between the two solutions to cross the cell rapidly. All concentrations are given in mM.

Internal A: Cs acetate 150.0, CsCl 10.0, TEA acetate 5.0, $MgCl_2$ 2.0, $CaCl_2$ 0.1, EGTA 1.1, HEPES 10.0.

Internal B: Cs acetate 135.0, CsCl 5.0, $MgCl_2$ 2.0, $CaCl_2$ 0.1, EGTA 1.1, HEPES 10.0.

Both internal solutions were adjusted for a pH of 7.4 with CsOH, and brought to an osmolarity of 270–290 mOsm which required dilution of Internal A. Internal solutions were filtered through a 0.2 μm syringe filter before use. To make pipette solutions for perforated-patch recordings, 1 ml of internal solution was added to a 4 μl aliquot of nystatin

Received July 12, 1994; revised Nov. 16, 1994; accepted Dec. 2, 1994.

This work was supported by EY04112 to M.W. We thank David Attwell, Andrew Ishida and Matt Frerking for their comments on this work and Richard Nuccitelli for help with Ca^{2+} imaging. We thank SmithKline Beecham pharmaceuticals for the gift of SKF 89976A.

Correspondence should be addressed to Martin Wilson, Division of Biological Sciences, Storer Hall, Davis, CA 95616.

[a]Present address: Department of Biology, University of California at San Diego, La Jolla, CA 92037.

(50 mg/ml in DMSO, Sigma) and an 8 μl solution of Pluronic F-127 (25 mg/ml DMSO, Molecular Probes) for a final nystatin concentration of 200 μg/ml. The mixture was well vortexed, sonicated for 30 sec, and stored on ice in the dark. Fresh nystatin internal solutions were made every 2 hr.

Normal external: NaCl 116.7, KCl 5.3, TEA Cl 20.0, $CaCl_2$ 3.0, $MgCl_2$ 0.41, glucose 5.6, HEPES 3.0.

0 K external: NaCl 122.2, TEA Cl 20.0, $CaCl_2$ 3.0, $MgCl_2$ 0.41, glucose 5.6, HEPES 3.0.

Low Cl external: KCl 5.3, Na isethionate 122.2, TEA Cl 20.0, $CaCl_2$ 3.0, $MgCl_2$ 0.41, glucose 5.6, HEPES 3.0.

100 Na-3 Ca external: NaCl 100.0, TEA Cl 20.0, $CaCl_2$ 3.0, $MgCl_2$ 0.41, glucose 5.6, HEPES 3.0; sucrose was added to adjust the osmolarity.

100 Na-10 Ca external: NaCl 100.0, TEA Cl 20.0 $CaCl_2$ 10.0, $MgCl_2$ 0.41, glucose 5.6, HEPES 3.0.

Ba external: normal external but with 3 mM $BaCl_2$ replacing 3 mM $CaCl_2$.

NMG Cl external: normal external but with a complete replacement of NaCl by NMG Cl.

Li external: normal external but with a complete replacement of NaCl with LiCl.

10 K external: NaCl 100.0, KCl 10.0, TEA Cl 20.0, $CaCl_2$ 3.0, $MgCl_2$ 0.41, glucose 5.6, HEPES 3.0.

0.1 K external: NaCl 100.0, KCl 0.1, TEA Cl 20.0, $CaCl_2$ 3.0, $MgCl_2$ 0.41, glucose 5.6, HEPES 3.0. The osmolarity was adjusted with sucrose.

One millimolar Na_3VO_4 solution was prepared in normal external immediately prior to use. All solutions were adjusted to a pH of 7.4 and contained 300 nM tetrodotoxin to block Na^+ channels and 10 μM bicuculline to block $GABA_A$ currents arising from autapses (Gleason et al., 1993). All experiments were done at room temperature (22–25°C). Cells were loaded with BAPTA by incubation with 10 μM BAPTA-AM for 1–2 hr at 37°C in culture medium. The final cytosolic concentration of BAPTA was unknown. All drugs applied were added to the external solution used, and delivered through the same inlet pipe via a manual switch in the gravity-flow apparatus.

Fura-2 ratio imaging

An imaging system similar to the one described by Tsien and Harootunian (1990) was used for measuring intracellular free $[Ca^{2+}]$ by the method of ratio imaging of fura-2 (Grynkiewicz et al., 1985). Details of the method used have been described elsewhere (Gleason et al., 1992), but with the following modifications: external solution B, which was used for the electrophysiological recordings in the vanadate experiments, was also used in the imaging experiments. All measurements were made at room temperature as were the electrophysiological experiments.

Electrophysiological recording

For recording, the culture dish was mounted on the stage of a Nikon inverted microscope and the cells visualized with phase-contrast optics. Patch electrodes were pulled from thick-walled borosilicate glass (1.5 mm o.d., 0.86 mm i.d.; Sutter Instruments, Novato, CA) on a Flaming-Brown pipette puller (Sutter Instruments). When measured in the bath, the pipettes had resistances of between 3 and 5 MΩ. Grounding of the dish was through an Ag/AgCl pellet in a saturated KCl well, connected to the dish via an agar bridge of saturated KCl, positioned downstream from the recorded cell. Junctional voltages between the pipette and external solutions have not been corrected for since an additional and unknown potential exists across the perforated patch (Horn and Marty, 1988). Rapid solution changes in which Na^+_o was replaced with either NMG or Li^+, because they gave rise to boundaries between the test solution and the bulk solution, could also generate voltages. For Li^+ these were found to be between 1 and 2 mV but for NMG, junctional voltages were too small to measure. The small junctional voltage generated by Li^+ solutions would be expected to shift the activation curve in the opposite direction to that shown in Figure 9. Data were acquired using an Axopatch 1D amplifier (Axon Instruments, Foster City, CA) and usually filtered at 1 kHz. Amacrine cells free from contact with other cells were chosen for recording. Gigaohm seals were achieved by briefly hyperpolarizing the pipette to around −90 mV then holding the voltage at −70 mV. Series resistance values were initially high (>100 MΩ) but within about 5 min fell to around 50 MΩ. Values were monitored throughout each experiment. Series resistance compensation was not generally used but where appropriate (e.g., Fig. 1*B*) steady state voltage errors were corrected based on measured currents and series resistance. To satisfy ourselves that our perforated patch method was not inadvertently causing rupture of the patch we conducted some early experiments with fluorescein in the pipette. Only in those rare instances where a sudden large drop in access resistance unambiguously indicated patch rupture was fluorescence seen in the cell.

Results

Ca^{2+} influx produces a slow tail current

Single, isolated amacrine cells were identified on morphological criteria (Gleason et al., 1993) and voltage clamped in the perforated patch configuration. With blockers of Na^+, K^+ and transmitter-gated channels, voltage-clamp records showed a voltage-dependent inward current that began to activate at about −50 mV. This inward current was identified as a Ca^{2+} current because it could be carried by Ba^{2+} and was blocked by Co^{2+} or Cd^{2+}. Calcium currents were sensitive to dihydropyridines, described in greater detail elsewhere (Gleason et al., 1994), and generally had peak values between 100 and 400 pA for steps to 10 mV (Fig. 1). For cells having maximum Ca^{2+} currents greater than about 50 pA, a tail current lasting hundreds of milliseconds could be seen on stepping back to a holding voltage of −70 mV (Fig. 2*A*).

Under the same recording conditions as described in Figure 2, the maximum tail current had a mean value of −19 ± 8 pA (±SD, n = 21 cells). The amplitudes of the tail currents were correlated with the amplitudes of the preceding Ca^{2+} current. The largest tail current followed the largest Ca^{2+} current (Fig. 2*A*). When the net charge moved during a tail was plotted against the previous voltage step, the relationship showed the same general form as the dependence of Ca^{2+} currents upon voltage (compare Figs. 1*B*, 2*B*). A small point of difference between the two curves is that tail currents go to zero at about 50 mV (Fig. 2*B*) whereas current, in most cells, becomes outward between 30 and 40 mV (Fig. 1*B*). A possible explanation for this is that Cs^+ is finitely permeant through Ca^{2+} channels, resulting in zero net current at potentials permitting net Ca^{2+} influx. The close relationship between tail size and Ca^{2+} current suggests that tail currents depend on Ca^{2+} influx.

What ions carry the tail current?

Two methods were used to examine the dependence of the tail current upon internal Ca^{2+}. In the first, currents were examined in normal external Ca^{2+} (3 mM) then with a complete replacement of Ca^{2+} with Ba^{2+}. Although Ba^{2+} carried a larger inward current during the voltage step, the slow tail current was abolished (Fig. 3*A*; n = 12), indicating that Ba^{2+} was unable to substitute for Ca^{2+} in activating this current. We also tested the dependence of the tail current on a rise in internal Ca^{2+} by preloading cells with the fast Ca^{2+} buffer, BAPTA, by incubation

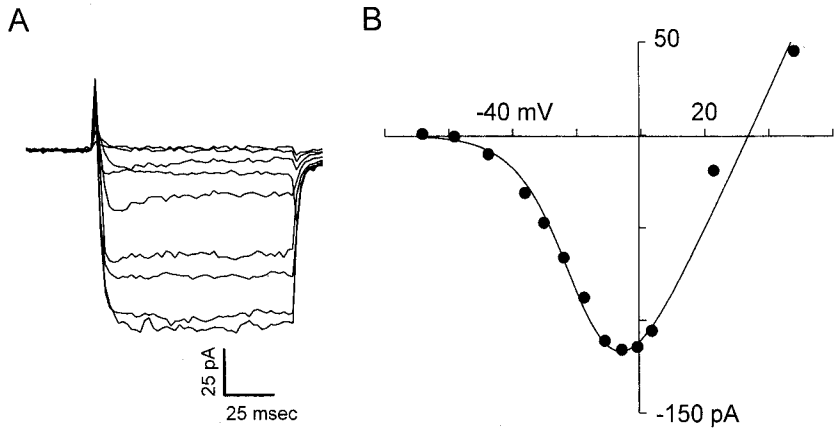

Figure 1. Calcium currents recorded from an amacrine cell. *A*, A family of Ca^{2+} currents elicited with 100 msec voltage steps ranging from −60 to +20 mV from a holding voltage of −70 mV. This cell was recorded in 0 mM K^+ external solution and internal solution B. Cells varied in their degree of inactivation with the cell illustrated showing very little. *B*, Calcium current amplitude measured 15 msec after the beginning of the voltage step, plotted against step voltage. The *I–V* plot includes data from current traces not shown in *A* and has been fitted with a function of the form $I = c(1 + \exp -(V - a/b))^{-1} (V - d)$. The points in *B* have been corrected for junction potential, linear leak, and series resistance error.

in its acetoxymethyl ester form. Tail currents were absent from BAPTA-loaded cells having Ca^{2+} currents of a size sufficient to generate tail currents in untreated cells (Fig. 3*B*; $n = 4$ cells). This suggests that elevated cytosolic Ca^{2+} is required to produce a tail current.

Although K^+ currents were largely blocked by inclusion of Cs^+ in the pipette and TEA in the external solution, external K^+ (5 mM in initial experiments) could potentially carry an inward current. A comparison of tails recorded in 0, 5, and 10 mM K^+ revealed (5 of 7 cells) a small inward current lasting about 100 msec as a component of the tail (Fig. 4*A*). To avoid this small contamination completely, most subsequent experiments were performed in zero external K^+.

To minimize contaminating Cl^- currents, recording solutions were designed to match the equilibrium potential for Cl^- to the holding potential (−70 mV) however an unknown potential across the perforated patch is likely to have made this match imperfect (Horn and Marty, 1988). When tail currents recorded at −70 mV in normal and low external Cl^- were compared, some cells (Fig. 4*B*, 2 of 5) showed small differences attributable to Cl^- current, that lasted around 100 msec. Neither of these small conductances could account for the prolonged tail current.

The effects on the tail current of changing external Ca^{2+} concentration was also examined. Calcium and tail currents were recorded in normal (3 mM Ca^{2+}) and 10 mM Ca^{2+} external solutions (Fig. 4*C*) and as expected, the magnitude of the Ca^{2+} current increased with higher external Ca^{2+}. In contrast, however, the tail currents in 10 mM Ca^{2+} were smaller and lasted longer than those recorded in the same cell with 3 mM Ca^{2+} externally. This result is not easily consistent with a Ca^{2+}-gated channel current but would be compatible with electrogenic Na-Ca exchange if, as shown elsewhere, the rate of Na-Ca exchange is reduced in high external Ca^{2+} (Hodgkin and Nunn, 1987). Consistent with this conclusion is our observation that tail currents are not associated with a noticeable increase in current noise (see, e.g., Fig. 7*B*). Since ouabain (100 μM) was without effect on the slow tail current ($n = 3$ cells), a contribution of the electrogenic Na-pump to the tail was ruled out. Cultured amacrine cells release GABA in a Ca^{2+}-dependent way (Gleason et al., 1993), and it might therefore be supposed that electrogenic GABA uptake could contribute to the tail current. This is not the case since the GABA uptake inhibitors ± nipecotic acid (1 mM, $n = 8$ cells; Fig. 5*A*) and SKF 89976A (Ali et al., 1985) (20 μM, $n = 5$ cells, data not shown) were without effect on tail currents.

By definition, Na-Ca exchange requires external Na^+ for

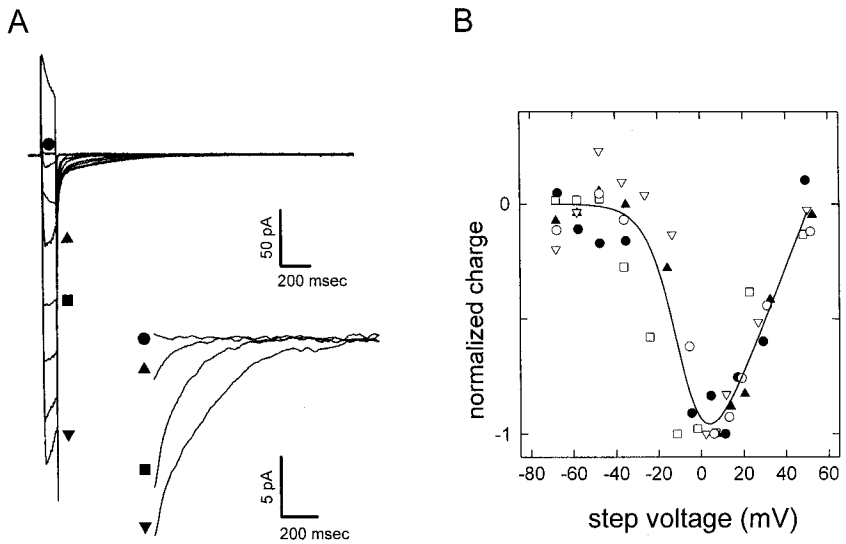

Figure 2. A long tail current follows the Ca^{2+} current. *A*, Calcium current in a representative cell was elicited from −70 mV with 100 msec voltage steps ranging from −60 to +60 mV. A prolonged inward tail current (lasting about 870 msec in this cell) is seen after the voltage step. *Inset*, Four of the tail current traces from *A* are shown at higher gain after smoothing by window averaging. Symbols indicate matching Ca^{2+} currents and tails. Record obtained using internal A and normal external solution. *B*, For five cells, subject to the same protocol as in *A*, tail currents have been integrated to yield charge. Charge values were normalized (to −1) for each cell and plotted against step voltage. The first 50 msec have not been included in this integral to avoid contamination by residual channel currents. The *solid line* shows a best fit function of the same form as in Figure 1*B*.

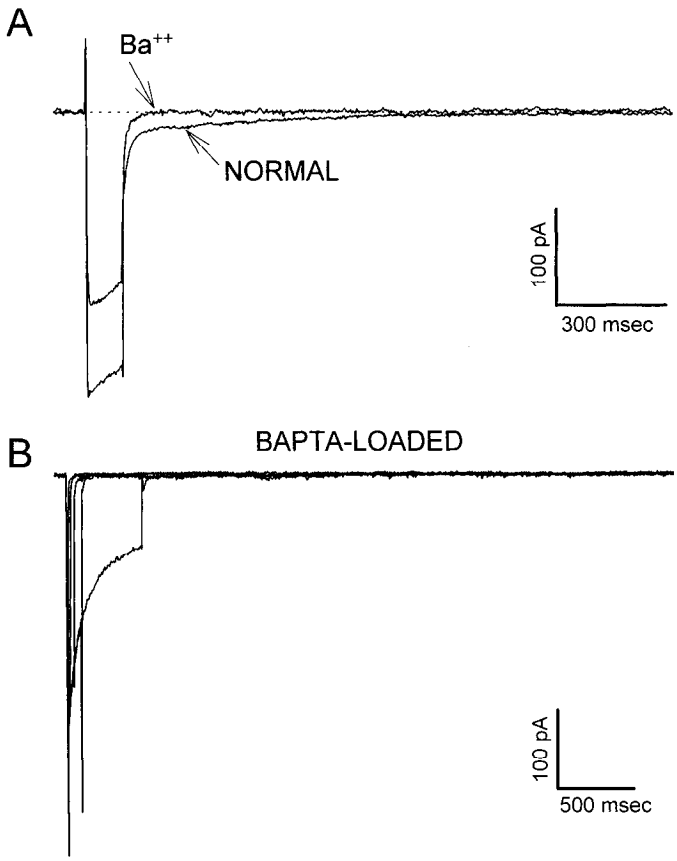

Figure 3. Slow tail requires elevated $[Ca^{2+}]_i$. *A*, A Ca^{2+} current and subsequent tail current are elicited by a step from −70 mV to 0 mV with either normal or Ba^{2+} external solution. Replacing Ca^{2+} with Ba^{2+} augments the voltage-gated current but abolishes the tail current. Internal solution B used. The *dotted line* denotes 0 pA. *B*, Currents in a BAPTA-loaded cell. In 0 mM K^+ external, steps from −70 mV to 0 mV for 10, 25, 50, 100, and 500 msec elicit Ca^{2+} currents but no tail currents.

which Li^+, though readily permeant through Na^+ channels (Hille, 1972), is unable to substitute (Blaustein, 1977). When external Na^+ was replaced with either the large impermeant cation *N*-methyl-D-glucamine (NMG) or Li^+ (Fig. 5*B*), the slow tail current was abolished. The abolition of the tail current was immediate upon replacement of solution around a neuron and was immediately and completely reversible. In order to examine what fraction of the tail current was attributable to Na-Ca exchange and what fraction to other contaminating, Li^+-insensitive currents, we compared tail currents elicited by voltage steps of different durations in either Na^+ or Li^+ containing solutions. With the exception of the 50 msec immediately following repolarization, removal of external Na^+ abolished nearly all tail current (Fig. 5*B*). Of nine cells examined quantitatively, the peak tail current in Li^+, excluding the first 50 msec, although much smaller than in Na^+, did increase with step length (Fig. 6*A*). These Li^+-insensitive currents probably represent, as expected, contaminating channel currents rather than exchange current spared by Li^+ since they were considerably briefer than exchange currents seen in Na^+. A measure of the contribution of contaminating currents to tail currents seen in Na^+ is provided by a comparison of time integrals of tail currents (Fig. 6*B*). For step durations greater than 50 msec, tail charge moved in Li^+ was less than 4.3% (mean of nine cells) of tail charge in Na^+, reaffirming the idea that almost all slow tail current is due to Na-Ca exchange.

As shown in Figure 6*C* the time course of the Li^+-sensitive current, determined by subtracting the tail in Li^+ from that in Na^+, is not greatly different from the unsubtracted tail current. Two points are clarified in the subtracted records though. First, as suggested by previous figures (e.g., Fig. 4*C*), exchange current saturates. Since contaminating currents are eliminated by this subtraction procedure we may conclude that saturation is a real property of the exchanger and not an artifact. Second, 10 msec voltage steps can clearly generate exchange currents. The possibility of contaminating currents in the first 50 msec following a Ca^{2+} current would make this result uncertain without the subtraction procedure.

Changes in $[K]^+_o$ have no effect on exchange

Two forms of Na-Ca exchange have been described in vertebrate cells. One form, demonstrated in heart muscle (Reeves and Hale, 1984), has a stoichiometry of $3Na^+:1Ca^{2+}$ whereas a form in rod outer segments transports $1Ca^{2+}$ and $1K^+$ out for every $4Na^+$ entering (Cervetto et al., 1989). With an exchange mechanism that transports K^+, the equilibrium Ca^{2+} concentration depends on the K^+ gradient as well as the Na^+ and Ca^{2+} gradients. In most experiments described thus far, K^+ has been omitted from both pipette and external solutions so as to avoid contaminating channel currents. This does not, however, exclude the possibility of exchange having rod outer segment stoichiometry since Cs^+, the major cation in the pipette solution, might substitute for K^+. An experiment to discover if K^+ is transported is illustrated in Figure 7*A*.

In this experiment a neuron without any imposed Ca^{2+} load, was suddenly switched from a solution containing 10 mM K^+ to one containing 0.1 mM K^+, and back again. If K^+ were cotransported with Ca^{2+}, this regime would be expected to produce a transient inward current as Ca^{2+} is expelled to reach the new equilibrium value for $[Ca^{2+}]_i$ and a subsequent transient outward current following the restoration of 10 mM K^+ (Cervetto et al., 1989). In order to increase any effect of changing K^+ concentration, the Na^+ gradient was lessened in these experiments by including 10 mM Na^+ in the patch pipette. No cells examined showed reversible transient currents that would indicate the transport of K^+ (Fig. 7*A*; $n = 11$ cells). In similar experiments, Ca^{2+} loads were imposed just prior to reduction of external K^+ to increase the difference between the cytosolic Ca^{2+} concentration and the new equilibrium concentration of Ca^{2+} (not shown). No effect of K^+ concentration was seen for these experiments either ($n = 3$ cells).

The ratio of calcium influx to calcium efflux

The stoichiometry of exchange has been productively examined in rods through an accounting of charge entering the outer segment during and after a calcium load (Yau and Nakatani, 1984; Hodgkin and Nunn, 1987; Cervetto et al., 1989; Lagnado and McNaughton, 1991). We have tried a similar approach in our cells. The basis for the approach is as follows. If, as indicated above, K^+ is not transported with Ca^{2+}, then the ratio of charge entering as Ca^{2+} current to the net current entering during the tail, and carried by Na^+, should reflect exchange stoichiometry. The ratio (r) of charges moved ($Q_{load}/Q_{exchange}$) is related to the number of Na^+ ions transported (n) per Ca^{2+} ion expelled, by the equation $r = 2/(n - 2)$.

Estimates of n were obtained in experiments using two dif-

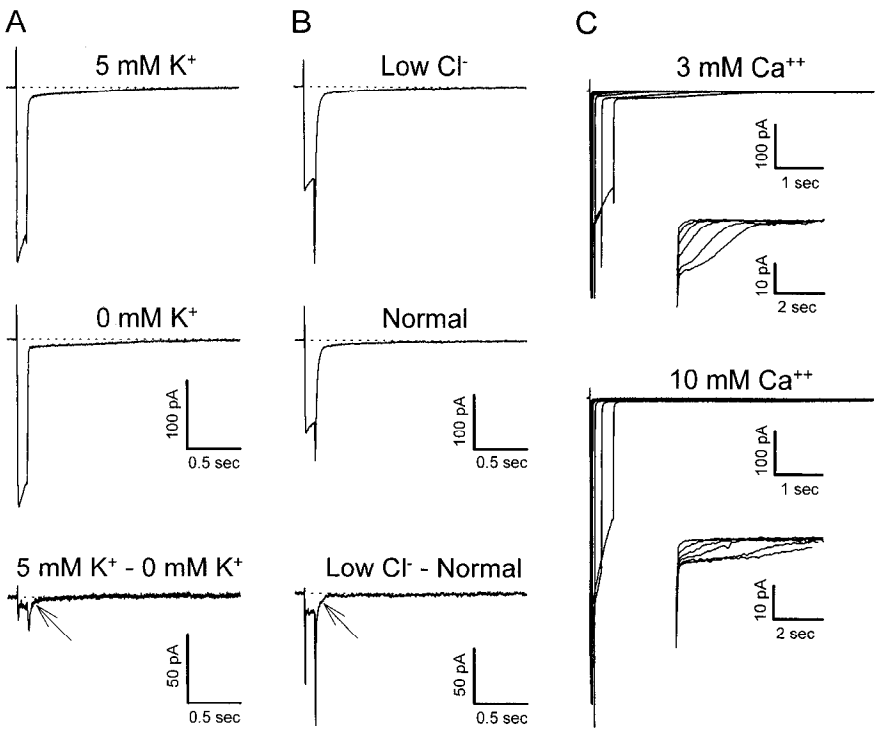

Figure 4. Ionic composition of the tail current. *A*, A Ca^{2+} current and subsequent tail current are elicited using the voltage protocol described for Figure 3*A* with internal B and either 5 mM K^+ (normal) external or 0 mM K^+. The *dotted line* denotes 0 pA. The *bottom trace* is a subtraction of the 0 mM K^+ record from the 5 mM K^+ record with an *arrow* indicating that a small inward current carried by K^+ ions contributes to the tail. *B*, Current records are shown from another cell using the same voltage protocol as A with internal B and either normal (149 mM Cl^-; $E_{Cl} = -70$ mV) external or low Cl^- (32 mM; $E_{Cl} = -31$ mV) external. The *bottom trace* is a subtraction of the current in normal Cl^- from that in low Cl^-. *Arrow* indicates a Cl^--dependent tail current. *C*, Two sets of current records are shown from the same cell. Steps from a hold of −70 mV to 0 mV, for 10, 25, 50, 100, 250, and 500 msec generate a family of Ca^{2+} and tail currents. The external solution for the upper family of traces is 100 mM Na^+, 3 mM Ca^{2+} and in the lower family of traces, 100 mM Na^+ and 10 mM Ca^{2+}. An increase in external Ca^{2+} concentration augments the Ca^{2+} current but the tail currents are reduced in amplitude and are prolonged.

ferent voltage protocols. In five cells stepped to the same voltage for different times (Fig. 7*B*), r had a mean value of 3.31 ± 0.87 (± SD) as determined from linear regression of plots like Figure 7*B*. These r values indicate an apparent stoichiometric ratio of 2.6Na^+:1Ca^{2+} and large variability between cells. Cells stepped to different voltages (Fig. 2*A*) had a mean r of 3.72 ± 1.0 (± SD, $n = 6$) giving an apparent stoichiometric ratio of 2.5 Na^+:1 Ca^{2+}. The apparent stoichiometry in all neurons was fewer than 3 Na^+ for every Ca^{2+} although this is the demonstrated stoichiometry in cardiac myocytes (Reeves and Hale, 1984) and is suggested for other preparations (reviewed in Eisner and Lederer, 1989).

Two sources of error that might bias our estimates of stoichiometry in our experiments require consideration. First, contamination of either the Ca^{2+} current or the tail current with residual channel currents could affect these estimates. Based on current records like those shown in Figure 4*B* and charge measurements as shown in Figure 6*B*, we estimate charge measurement errors due to contaminating currents to be less than 10%. A second source of error would result if the exchanger were working during the voltage step. In this circumstance a fraction of the Ca^{2+} entering would be cleared before the end of the step and therefore not appear as tail current. Any inward exchange current generated during the step would be erroneously accounted as calcium load and further compound the error.

In order to estimate the magnitude of this error we would need to know the, presently unknown, voltage dependence of the exchange current. In other cells exchange current has been found to have an exponential dependence on voltage (Kimura et al., 1987; Lagnado et al., 1988) with the exponent a function of ion concentrations (Lagnado et al., 1988). If we assume, as a worst case, that exchange current is of similar size at 0 mV and −70 mV then substantial errors could be created in cells having relatively large tails (e.g., Fig. 7*B*), though not in those cells having small tails. The situation would be made more complicated if exchange stoichiometry were not fixed but depended on voltage or ion concentrations. Fortunately, the evidence argues against large errors.

The exchanger removes little calcium during a voltage step

We have examined experimentally the issue of exchange during the voltage step by comparing Ca^{2+} currents measured in the presence or absence of Na^+ and by examining tail currents following Ca^{2+} loaded in the presence or absence of Na^+. If Na-Ca exchange were substantial during the voltage step then "Ca^{2+} currents" in Na^+ should be larger than in the absence of Na^+ by an amount equal to the exchange current. Tail currents, measured in Na^+, following a calcium load in Na^+ ought, conversely, to be smaller by an amount equivalent to the Ca^{2+} exchanged during the step.

To carry out these experiments, cells were stepped rapidly from Na^+ containing solution to one in which Na^+ was replaced with either Li^+ or NMG. Most of these experiments were carried out using NMG because its higher refractive index allowed easy discrimination of the boundary between the two streams of flowing liquid. NMG, and to a lesser extent Li^+, generated an outward current when applied to cells held at −70 mV. This current chiefly represents a reduction in the inward leak current and is unconnected with the exchange current since it was seen when Ba^{2+} replaced external Ca^{2+}. Appropriate leak corrections have been made for these two solutions.

When matched voltage steps were applied alternately with and without Na^+, steps to voltages negative to 0 mV consistently generated larger currents in Na^+ than in NMG or Li^+. This result might suggest a contribution of exchange current to the inward current seen in Na^+ but, in fact, its explanation lies in a small

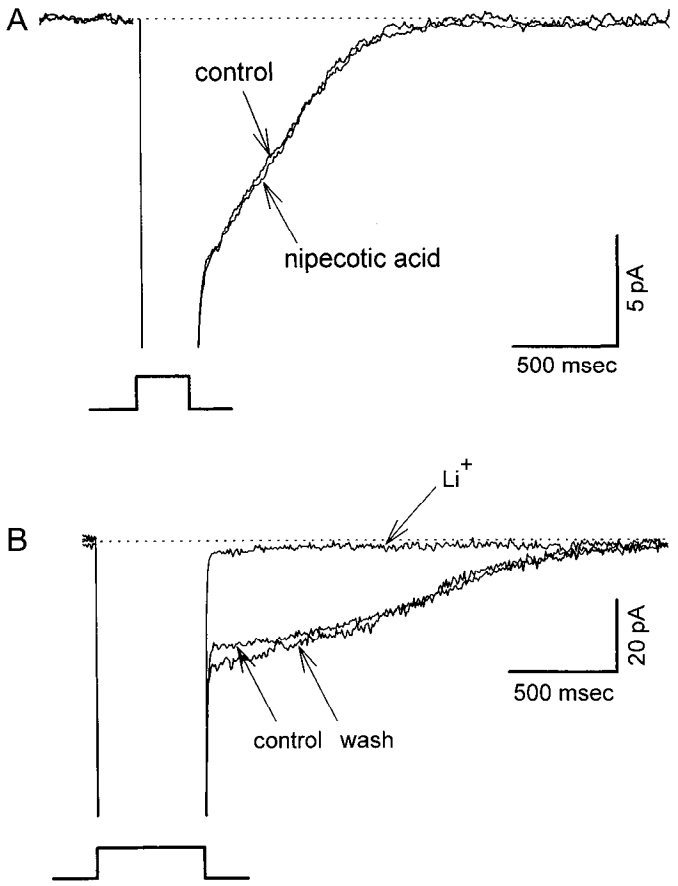

Figure 5. The effect of nipecotic acid and Li^+ on the tail current. *A*, Tails in an amacrine cell, elicited by a 250 msec step to 0 mV from −70 mV in normal external solution and in the presence of nipecotic acid (1 mM). The tail current following the step to 0 mV was unchanged when the cell was superfused with nipecotic acid. Traces represent the average of six records in nipecotic acid and in the control record, the average of six records before and six following nipecotic acid application. *B*, Current tails from another amacrine cell held at −70 mV and stepped to 0 mV for 500 msec, in normal Na^+-containing external solution, before and after replacement of Na^+ with Li^+. Tail currents are almost completely suppressed in Li^+.

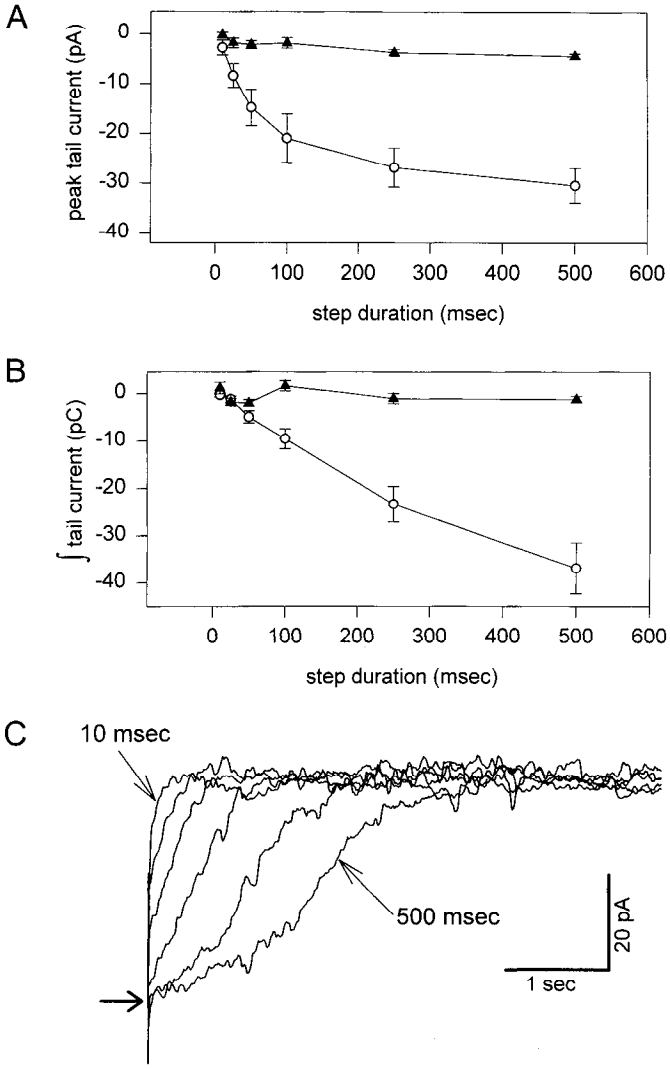

Figure 6. Dependence of Na^+-dependent tail currents on the duration of the voltage step. *A*, Mean tail currents measured 50 msec after the end of steps to 0 mV lasting 10, 25, 50, 100, 250, and 500 msec (n = 9 cells, ±SE). In the presence of Li^+ (*solid triangles*), the peak tail current is small (<5 pA) compared to the normal peak current (*open circles*) which is near saturation at approximately 30 pA. *B*, Tail currents obtained for the same cells as in *A* were integrated between 50 msec following the end of each voltage step and approximately 3–4 sec following the step, at which time currents had all decayed to zero (n = 9, ±SE). The integrated current, that is, the charge in the tail current is plotted against step duration. When Li^+ (*solid triangles*) replaced Na^+ (*open circles*) in the superfusing solution, virtually no tail charge was moved. *C*, Tail currents obtained for one cell by subtracting the tails in Li^+ from those seen in Na^+. Tails have all been aligned to the end of voltage step and represent tails elicited by steps of 10, 25, 50, 100, 250, and 500 msec duration. The initial currents elicited by the 250 and 500 msec steps show saturation (*arrow*).

shift in the Ca^{2+} current activation curve. Using voltage ramps as a way to describe the entire *I–V* relation as in Figure 9, it is clear that a rightward shift of a few mV in the absence of Na^+ (mean = 5.71 mV in Li^+, n = 5 cells; mean = 5.48 mV in NMG, n = 9 cells) can explain the discrepancy in measured current. A similar shift was seen in Ba^{2+} (Fig. 9*B*), removing the possibility of the involvement of the exchanger. With the exception of slow, indirect effects (Balke and Wier, 1992), Na^+ has not been reported to have effects on Ca^{2+} currents, so we are unable to ascribe our observation to any known mechanism. Although its location on the voltage axis was shifted (Fig. 9), no consistent difference was seen in the maximum inward current elicited with or without external Na^+. This implies that exchange current makes no observable contribution during this voltage regime but leaves open the possibility that Ca^{2+} accumulation during a step of voltage might be sufficient to cause significant exchange. A comparison of tail currents makes this appear unlikely though.

Charge moved in tail currents following calcium loads in alternating Na^+ or NMG solutions was calculated by integrating tail currents as before. In order to remove the effects on the leak current seen in NMG, a control record having no voltage step was subtracted from the test record, as shown in Figure 10. In four cells examined in detail, loads acquired with Na^+ present produced tails that were slightly, but significantly ($p < 0.001$, Wilcoxon signed rank test) larger than those resulting from a load acquired in the absence of Na^+. Tails from the load in NMG were, on average, 89.9% of those resulting from loads in Na^+. We suspect this difference is due to a small loss of Ca^{2+} load between the end of the voltage step and the return from NMG to Na^+ solution (Fig. 10*C*).

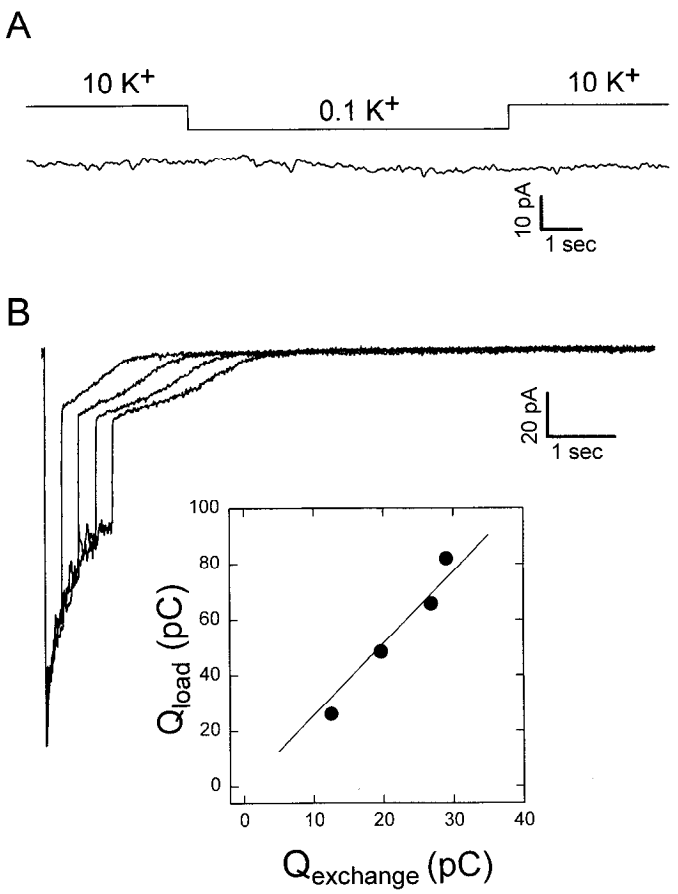

Figure 7. Stoichiometry of the Na-Ca exchanger. *A*, Currents recorded from an amacrine cell held at −70 mV suddenly changed from 10 mM K^+ external solution to 0.1 mM K^+, and back. Fluctuations in current of a few pA, partly due to residual ion channel currents and characteristic of records made with 10 mM internal Na^+, are seen in this cell. Transient currents at solution changes, that would indicate the transport of K^+ by an exchanger, did not occur. *B*, Current records from a cell held at −70 mV and stepped to 0 mV for 250, 500, 750, and 1000 msec, recorded with internal B and 0 mM K^+ external containing 100 μM ouabain. Charge moved in the tail current, and carried by Na^+, ought to bear a stoichiometric relation to the charge entering during the voltage step. This relationship is described in the *inset* by a plot of load charge (Q_{load}) against exchange charge ($Q_{exchange}$) and has a linear regression slope of 2.5, leading to an estimate of the stoichiometry as 2.8 Na^+:1Ca^{2+}. As was the case for most cells examined, the lowest ratio was given by the shortest step (r = 2.09) and the largest ratio by the longest (r = 2.82).

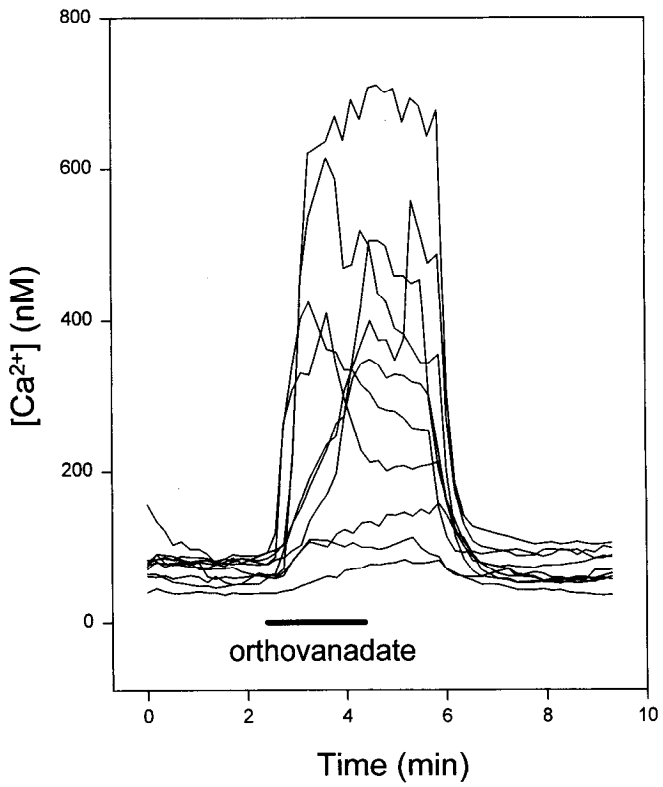

Figure 8. Effect of orthovanadate, an ATPase inhibitor, on cytosolic Ca^{2+} concentration in amacrine cells. Ca^{2+} concentration is shown for 10 cell bodies within a single field as estimated by ratio imaging of Fura-2. Application of orthovanadate caused a general increase in Ca^{2+} from a baseline level of 65 nM ± 23 SD to 392 nM ± 216 SD. The delay in onset of this increase and the delay in its fall following removal of orthovanadate is not accounted for by delay in solution changes but is probably due to entry and efflux of orthovanadate across the cell membrane.

From the foregoing experiments we conclude that Na-Ca exchange is not significant during the voltage step. As a consequence we think it likely that the failure of experiments like those in Figure 7*B* to reveal a consistent stoichiometry is the result of Ca^{2+} removal by processes other than Na-Ca exchange.

The fraction of Ca^{2+} removed by Na-Ca exchange

The large variance in the calculated r values represents consistent and repeatable differences between cells, some of which had relatively large tail currents and others of which did not. For those traces, like the 250 msec step in Figure 7*B*, where r is close to 2, an exchanger with a stoichiometry of 3Na^+:1Ca^{2+} can account for virtually all clearance of the Ca^{2+} load. Where r values are higher, that is, tails are small relative to the Ca^{2+} load, other processes must be removing cytoplasmic Ca^{2+}. The relative importance of the exchanger in removing Ca^{2+} can be derived from our estimates of r. The mean fraction cleared by exchange, as determined by the two voltage protocols (Figs. 2*A*, 5*B*), was between 54% and 60%, assuming a stoichiometry of 3Na^+:1Ca^{2+}.

The remainder of the Ca^{2+} load must be either pumped out by the plasma membrane Ca^{2+}-ATPase, sequestered by organelles, buffered, or some combination of all three processes. The relative importance of Ca^{2+}-ATPases in clearing these Ca^{2+} loads was examined by incubating cells in orthovanadate, a potent inhibitor of ATPases including ion motive ATPases (Robinson, 1981; Pedersen and Carafoli, 1987). To check that externally applied vanadate would inhibit Ca-ATPases, amacrine cells were loaded with Fura-2 AM and internal Ca^{2+} concentration examined by ratio imaging (Gleason et al., 1992). Within 1 min of application, vanadate caused a rise in $[Ca]_i$, measured at the soma, from 65 ± 23 nM (±SD, n = 10 cells) to 392 ± 216 nM. Removal of vanadate was followed by a recovery to baseline after a delay of about 2 min (Fig. 8). These results demonstrate that ATPases, as expected, must play a major role in Ca^{2+} homeostasis in these neurons. For five neurons examined in normal external solution and then in normal plus orthovanadate, ratios of $Q_{exchange}$ to Q_{load} were determined by the same method used in Figure 7*B*. No significant differences ($p < 0.05$) were found in the two solutions (r = 3.63 ± 1.31, mean ± SD in normal; r = 3.65 ± 1.70 in vanadate), indicating that Ca^{2+}-

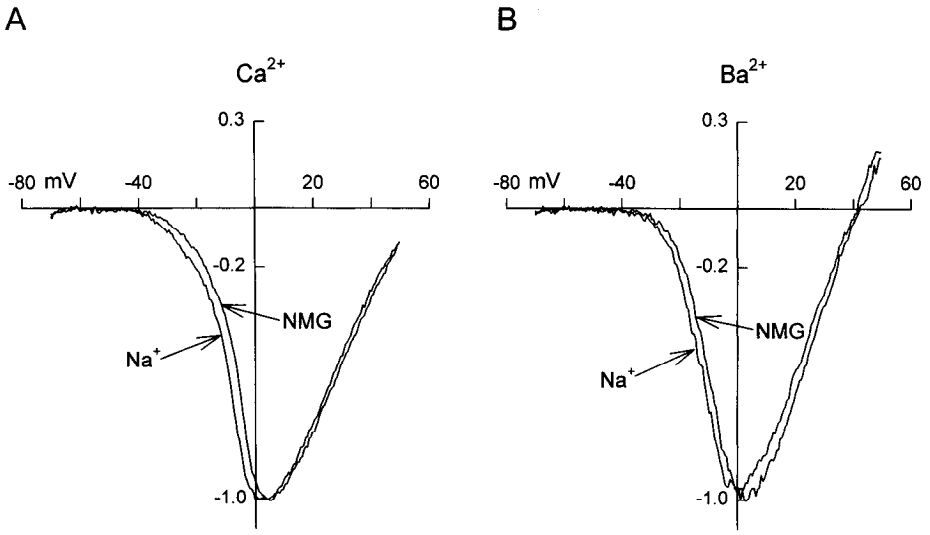

Figure 9. *I–V* relations determined in Na^+ and NMG solutions. *A*, 200 msec voltage ramps from −70 mV to +50 mV were used to generate these curves. A ramp in NMG was followed 3 sec later by a ramp in Na^+. A small rightward shift of the activating limb of the curve in NMG is apparent in this typical record. Controls showed that no shift was seen when solutions were not changed. *B*, Another cell examined as in *A* but having all external Ca^{2+} replaced by Ba^{2+}. In both *A* and *B*, peaks have been normalized. Actual peak currents in *A* were −136.3 pA in Na^+, and −134.4 pA in NMG. In *B*, the peak currents were −245.7 pA in Na^+ and −255.9 pA in NMG.

ATPases do not contribute significantly to the removal of Ca^{2+} loaded under these conditions.

The time course of calcium removal by other processes

By inhibiting plasmalemma Ca-ATPase with vanadate and preventing Na-Ca exchange by withholding external Na^+ we have examined the time course with which other processes remove Ca^{2+}. As shown in Figure 11, the experiment consisted of varying the delay between a calcium load in NMG solution and the return of external Na^+. As in Figure 10 a control record in NMG was subtracted from the test record to remove the change in leak current.

Eight cells were examined with the protocol shown in Figure 11 and all showed a decline in tail charge as exchange was delayed. The mean rate of Ca^{2+} removal, estimated by fitting data points with a linear regression was 31.5 ± 8.5% (mean ± SD) per second.

Discussion

Identification of electrogenic Na-Ca exchange in amacrine cells

The slow inward tail current we describe here is the result of electrogenic Na-Ca exchange which is stimulated by the influx of Ca^{2+} through voltage gated channels. Several pieces of evidence argue strongly in favor of this conclusion. Particularly crucial are the results showing that Ca^{2+} influx is required to elicit this current but that elevated external Ca^{2+} concentration diminishes the current amplitude while extending its time course. While Cl^- and K^+ ions are without effect at relatively long times after Ca^{2+} influx, Na^+ ions are required to support the tail current and Li^+, as in other preparations is unable to substitute. In the presence of Li^+, tail currents longer than about 50 msec are almost totally suppressed and lead us to estimate that less than 4.3% of the tail charge is not associated with the exchanger.

The exchanger clears a large fraction of Ca^{2+} load

The stoichiometry of the exchanger in amacrine cells is unknown but based on experiments like that shown in Figure 7*A* a stoichiometry involving K^+ seems less likely than one involving just Na^+ and Ca^{2+}. If we assume that a net, single charge is moved inward for every Ca^{2+} expelled, as is always the case in the rod outer segment (Lagnado et al., 1988; Lagnado and McNaughton, 1991) and is true for at least some conditions in cardiac myocytes (Reeves and Hale, 1984; Kimura et al., 1987), then we estimate that a substantial fraction, in most cells the majority, of Ca^{2+} load is removed by Na-Ca exchange. This inference stands in contrast of the conclusions drawn from work on cultured dorsal root ganglion neurons (Duchen et al., 1990; Thayer and Miller, 1990; Benham et al., 1992). In these studies, removal of external Na^+ was found to have little or no effect on the clearance of Ca^{2+} entering through voltage dependent Ca^{2+} channels. Differences in method may underlie this discrepancy. The studies mentioned above all employed fluorimetric measurements from cell bodies, whereas our approach examines the fraction of the total Ca^{2+} load expelled by the exchanger from all parts of the cell. Solely on the basis of surface-to-volume ratios, it is likely that Ca^{2+} loads will be handled differently by dendrites and cell bodies (Thayer and Miller, 1990) if as elsewhere (DiPolo and Beaugé, 1979, 1983), the membrane Ca^{2+} pump is a high affinity, low capacity system and the exchanger has low affinity but high capacity. As expected of this interpretation, rat brain synaptosomes examined fluorimetrically do show a strong dependence of internal Ca^{2+} concentration on external Na^+ (Nachshen, 1985).

The conclusion that a large fraction of a Ca^{2+} load in amacrine cells is cleared by an electrogenic exchanger has important implications for those processes employing Ca^{2+} as a messenger since it renders the persistence of elevated Ca^{2+} a function of membrane voltage and the Na^+ gradient. Among these processes is synaptic transmission which we have shown relies, in these neurons, on Ca^{2+} entry through channels like those described in Figure 1 and whose time course suggests that Ca^{2+} clearance is crucial in terminating release (Gleason et al., 1993). Preventing exchange by removing external Na^+ has been shown (Gleason et al., 1994) to dramatically extend the period of transmitter release.

Removal of Ca^{2+} by other processes

A striking feature of our results is the variability, between cells, in the ratio of charge moved during and after a voltage step. It is unlikely that errors in estimating Ca^{2+} load or efflux can account for this. In particular, experiments like that shown in Figure 10 rule out a substantial accounting error resulting from

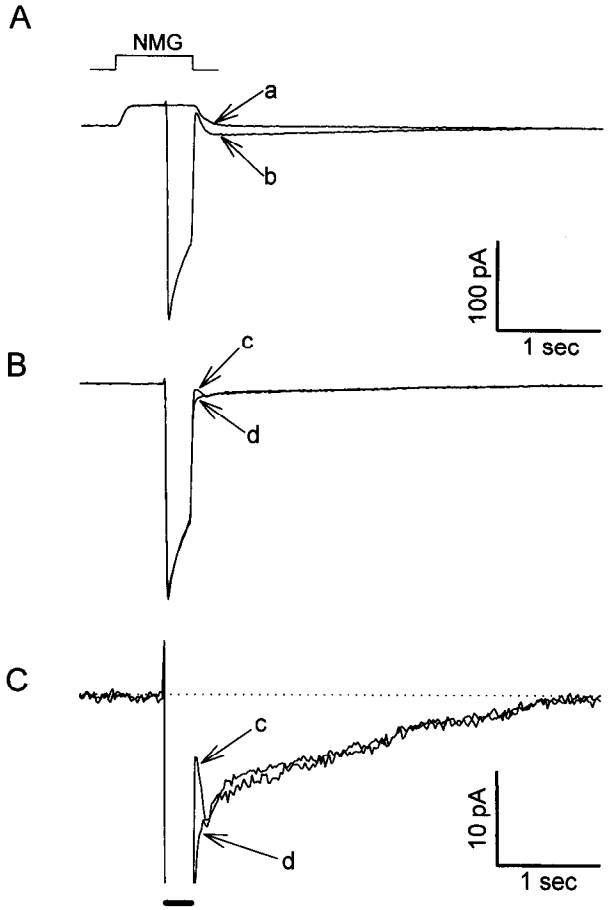

Figure 10. Tail currents following a calcium load in either Na^+ or NMG-containing solution. *A*, A pair of records (*a, b*) in which NMG solution was rapidly applied to the cell, as indicated by a step shown at the top. Record *b* shows Ca^{2+} current elicited by a voltage step, shown as a bar at the bottom of the figure, followed by a tail current beginning as the cell was switched back to Na^+-containing solution. Record *a* was a control without a voltage step, showing only the reduction in leak current produced by NMG. *B*, Record *a* has been subtracted from *b* to give *c*. Record *d* shows a Ca^{2+} current and tail measured in Na^+ containing solution throughout. To match Ca^{2+} currents exactly, the voltage was stepped to +10 mV for *c* and to 0 mV for *d*. *C*, Tail currents from *B* are shown enlarged. Tail currents are similar except that in *c*, the tail onset is slightly delayed by the noninstantaneous switching of solutions. One millimolar vanadate was present in both NMG and Na^+ solutions.

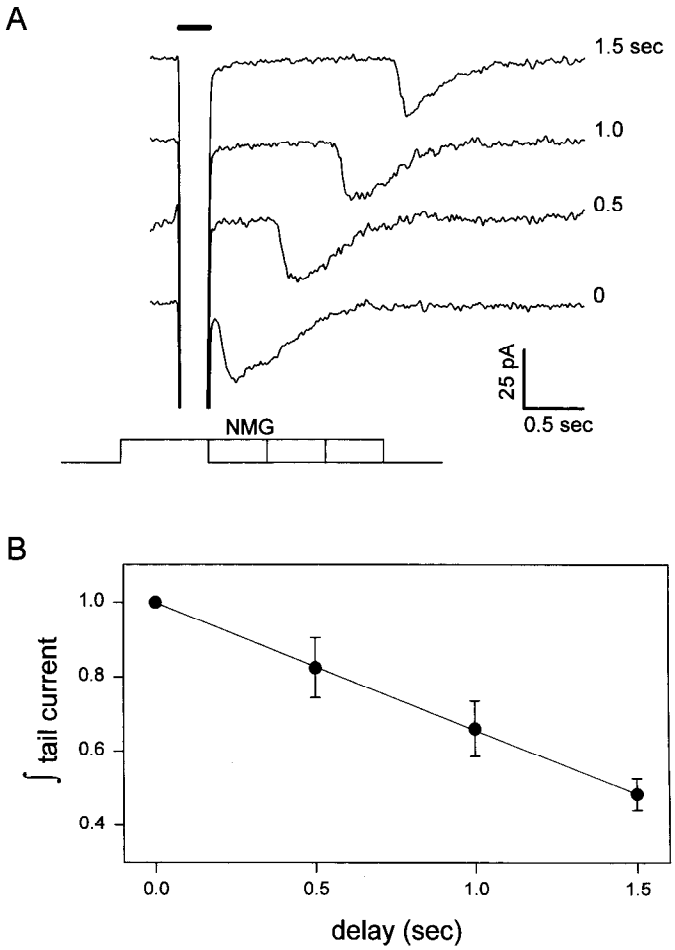

Figure 11. The effect of delayed restoration of external Na^+ on tail charge. *A*, Four records in which Ca^{2+} current was elicited by a step to +10 mV, indicated by the bar. Prior to and during the voltage step, Na^+ solution was replaced with NMG. As shown by the steps at the bottom of the panel, Na^+ solution was restored after a variable delay, indicated to the right of each trace, following the end of the voltage step. As in Figure 10*A*, each trace is the difference between a control trace and one having a voltage step. *B*, Tail integrals from multiple iterations of the protocol shown in *A* in which delays were presented in pseudorandom order. In each iteration of the protocol, tail charge was normalized to that of the 0 sec delay. Error bars show SDs and the *straight line* is a regression with a slope of 34.2% per second. One millimolar vanadate was present in the external solutions.

exchange during a voltage step. We think it unlikely that the observed variability originates in exchange stoichiometry varying between cells. Most probably, a variable fraction of Ca^{2+} load is removed by another mechanism. Ultimately, since it represents the only alternative mechanism for Ca^{2+} expulsion, the plasmalemmal Ca^{2+}-ATPase must remove the balance of Ca^{2+} load not cleared by the exchanger. In the short term though, our results argue that Ca^{2+} pumps are not important in clearing Ca^{2+} loads.

If Ca^{2+} pumps were important, then exchange tail currents should be augmented in the presence of vanadate. This was not found to be the case. In the presence of vanadate, the fraction of a Ca^{2+} load available to the exchanger decreased with time at a rate of about 30% per second. What process might be responsible for this removal of Ca^{2+}? Since vanadate acts intracellularly, it is probable, though by no means certain, that all ion-motive Ca^{2+}-ATPases, not just the plasmalemmal Ca^{2+}-ATPase, were inhibited in our experiments. Because uptake of Ca^{2+} into mitochondria depends instead on a proton gradient developed by the electron transport chain (Rottenberg and Scarpa, 1974), mitochondria are a possible candidate for the observed Ca^{2+} removal. Mitochondria are thought to play this role in other vertebrate neurons (Thayer and Miller, 1990). A plausible alternative though is that Ca^{2+} is simply able to diffuse away from Na-Ca exchanger molecules, though at a much slower rate than in free solution owing to the presence of cytosolic Ca^{2+} buffers (Fogelson and Zucker, 1985). Even assuming that the Na-Ca exchanger is uniformly distributed over the membrane, rather than concentrated at synapses (Luther et al., 1992), the relatively large volume of the cell body, for example, would represent a sink from which Ca^{2+} ions would emerge only slowly. Differences in shape between amacrine cells and differences in placement of their Ca^{2+} channels might account for the observed variability.

References

Ali FE, Bondinell WE, Dandridge PA, Frazee JS, Garvey E, Girard GR, Kais C, Ku TW, Lafferty JJ, Moonsammy GI (1985) Orally active and potent inhibitors of gamma-aminobutyric acid uptake. J Med Chem 28:653–660.

Balke CW, Wier WG (1992) Modulation of L-type calcium channels by sodium ions. Proc Natl Acad Sci USA 89:4417–4421.

Benham CD, Evans ML, McBain CJ (1992) Ca^{2+} efflux mechanisms following depolarization evoked calcium transients in cultured rat sensory neurones. J Physiol (Lond) 455:567–583.

Blaustein MP (1977) Effects of internal and external cations and of ATP on sodium–calcium and calcium–calcium exchange in squid axons. Biophys J 20:79–110.

Carafoli E (1991) Calcium pump of the plasma membrane. Physiol Rev 71:129–153.

Cervetto L, Lagnado L, Perry RJ, Robinson DW, McNaughton PA (1989) Extrusion of calcium from rod outer segments is driven by both sodium and potassium gradients. Nature 337:740–743.

DiPolo R (1989) The sodium–calcium exchange in intact cells. In: The sodium–calcium exchange (Allen TJA, Noble D, Reuter H, eds), pp 5–26. London: Oxford UP.

DiPolo R, Beaugé L (1979) Physiological role of ATP-driven Ca pump in squid axons. Nature 278:271–273.

DiPolo R, Beaugé L (1983) The calcium pump and sodium–calcium exchange in squid axons. Annu Rev Physiol 45:313–324.

Duchen MR, Valdeolmillos M, O'Neill SC, Eisner DA (1990) Effects of metabolic blockade on the regulation of intracellular calcium in dissociated mouse sensory neurones. J Physiol (Lond) 424:411–426.

Ehara T, Matsuoka S, Noma A (1989) Measurement of reversal potential of Na^+-Ca^{2+} exchange current in single guinea-pig ventricular cells. J Physiol (Lond) 410:227–249.

Eisner DA, Lederer WJ (1989) The electrogenic sodium-calcium exchange. In: The sodium–calcium exchange (Allen TJA, Noble D, Reuter H, eds), pp 178–207. London: Oxford UP.

Eliasof S, Barnes S, Werblin F (1987) The interaction of ionic currents mediating single spike activity in retinal amacrine cells of the tiger salamander. J Neurosci 7:3512–3524.

Fogelson AL, Zucker RS (1985) Presynaptic calcium diffusion from various arrays of single channels: implications for transmitter release and synaptic facilitation. Biophys J 4:1003–1017.

Gleason E, Mobbs P, Nuccitelli R, Wilson M (1992) Development of functional calcium channels in cultured avian photoreceptors. Visual Neurosci 8:315–327.

Gleason E, Borges S, Wilson M (1993) Synaptic transmission between pairs of retinal amacrine cells in culture. J Neurosci 13:2359–2370.

Gleason E, Borges S, Wilson M (1994) Control of transmitter release from retinal amacrine cells by Ca^{2+} influx and efflux. Neuron 13: 1109–1117.

Grynkiewicz G, Poenie M, Tsien RY (1985) A new generation of calcium indicators with greatly improved fluorescence properties. J Biol Chem 260:3440–3450.

Hille B (1972) The permeability of the sodium channel to metal cations in myelinated nerve. J Gen Physiol 59:637–658

Hodgkin AL, Nunn BJ (1987) The effects of ions on sodium–calcium exchange in salamander rods. J Physiol (Lond) 391:371–398.

Horn R, Marty A (1988) Muscarinic activation of ionic currents measured by a new whole-cell recording method. J Gen Physiol 92:145–159.

Huba R, Hoffmann H-D (1990) Identification of GABAergic amacrine cell-like neurons developing in chick retinal monolayer cultures. Neurosci Lett 117:37–42.

Katz B, Miledi R (1967) The timing of calcium action during neuromuscular transmission. J Physiol (Lond) 189:535–544.

Kimura J, Noma A, Irisawa H (1986) Na-Ca exchange current in mammalian heart cells. Nature 319:596–597.

Kimura J, Miyamae S, Noma A (1987) Identification of sodium–calcium exchange current in single ventricular cells of guinea-pig. J Physiol (Lond) 384:199–222.

Lagnado L, McNaughton PA (1989) The sodium–calcium exchange in photoreceptors. In: The sodium–calcium exchange (Allen TJA, Noble D, Reuter H, eds), pp 261–297. London: Oxford UP.

Lagnado L, McNaughton PA (1990) The electrogenic properties of the Na:Ca exchange. J Membr Biol 113:177–191.

Lagnado L, McNaughton PA (1991) Net charge transport during sodium-dependent calcium extrusion in isolated salamander rod outer segments. J Gen Physiol 98:479–495.

Lagnado L, Cervetto L, McNaughton PA (1988) Ion transport by the Na-Ca exchange in isolated rod outer segments. Proc Natl Acad Sci USA 85:4548–4552.

Luther PW, Yip RK, Bloch RJ, Ambesi A, Lindenmayer GE, Blaustein MP (1992) Presynaptic localization of sodium/calcium exchangers in neuromuscular preparations. J Neurosci 12:4898–4904.

McNaughton PA (1991) Fundamental properties of the Na-Ca exchange. An overview. Ann NY Acad Sci 639:2–9.

Mechman S, Pott L (1986) Identification of Na-Ca exchange current in single cardiac myocytes. Nature 319:597–599.

Nachshen DA (1985) Regulation of cytosolic calcium concentration in presynaptic nerve endings isolated from rat brain. J Physiol (Lond) 363:87–101.

Pedersen PL, Carafoli E (1987) Ion motive ATPases. Trends Biochem Sci 12:186–189.

Reeves JP, Hale CC (1984) The stoichiometry of the cardiac sodium–calcium exchange system. J Biol Chem 259:7733–7739.

Robinson JD (1981) Vanadate inhibition of brain (Ca + Mg)-ATPase. Neurochem Res 6:225–232.

Rottenberg H, Scarpa A (1974) Calcium uptake and membrane potential in mitochondria. Biochemistry 13:4811–4819.

Smith SJ, Augustine GJ (1988) Calcium ions, active zones and synaptic transmitter release. Trends Neurosci 11:458–464.

Thayer SA, Miller RJ (1990) Regulation of the intracellular free calcium concentration in single rat dorsal root ganglion neurones *in vitro*. J Physiol (Lond) 425:85–115.

Tsien RY, Harootunian AT (1990) Practical design criteria for a dynamic ratio imaging system. Cell Calcium 11:93–110.

Werblin FS, Dowling JE (1969) Organization of the retina of the mudpuppy. II. Intracellular recording. J Neurophysiol 32:339–355.

Yau K-W, Nakatani K (1984) Electrogenic Na-Ca exchange in retinal rod outer segment. Nature 311:661–663.